6- Tomita M, Osada T, Istvan S, Tomita Y, Unekawa M, Toriumi H, Tanahashi N, Suzuki N. Automated method for tracking vast numbers of FITC-labeled RBCs in microvessels of rat brain in vivo using a high-speed confocal microscope system. Microcirculation. 15: 163-174, 2008.

E．健康危険情報

該当なし

F．研究業績

1．論文発表

1. Unekawa M, Tomita M, Osada T, Tomita Y, Toriumi H, Suzuki N. Sampling rate-dependent RBC velocity in intraparenchymal single capillaries of rat cerebral cortex. Microvascular reviews and Communications. 1(1) : 12-15, 2007.

2. Tomita M, Osada T, Istvan S, Tomita Y, Unekawa M, Toriumi H, Tanahashi N, Suzuki N. Automated method for tracking vast numbers of FITC-labeled RBCs in microvessels of rat brain in vivo using a high-speed confocal microscope System. Microcirculation. 15(2): 163-174, 2008.

3. Tomita M, Osada T, Unekawa M, Tomita Y, Toriumi H, Suzuki N. Nitric oxide vanished capillary RBC in the face of an increase in arteriolar flow in the rat cerebral cortex. Microvascular reviews and Communications, in press.

2．学会発表

（国内学会）

1. 冨田裕、鳥海春樹、長田高志、冨田稔、畝川美悠紀、酒井宏水、土田英俊、堀之内宏之、小林紘一、鈴木則宏： マウス脳梗塞モデルへの人工赤血球投与の試み、第19回日本脳循環代謝学会総会、口演（平成19年10月盛岡)。

2. 長田高志、冨田稔、冨田裕、畝川美悠紀、鳥海春樹、鈴木則宏： 共焦点レーザー顕微鏡を用いたげっ歯小動物大脳皮質実質内毛細血管とグリア細胞および赤血球挙動の観察法、第19回日本脳循環代謝学会総会、口演（平成19年10月盛岡)。

3. 鳥海春樹、清水利彦、冨田稔、冨田裕、長田高志、畝川美悠紀、鈴木則宏： マウス頭蓋内静脈の生理的役割の研究、第35回日本頭痛学会総会、口演（平成19年11月東京)。

4. Toriumi H, Shimizu T, Tomita M, Tomita Y, Shibata M, Osada T, Gotoh K, Unekawa M, Tatarishvili J, Suzuki N: Decrease in velocities of FITC-labelled RBC flowing through diploic vein induced by local cooling. 第33回日本微小循環学会総会、口演（平成20年2月東京）

5. Unekawa M, Tomita M, Osada T, Tomita Y, Toriumi H, Tatarishvili J, Suzuki N: Effect of single capillary lengths in optically sliced thin layer of the rat cerebral cortex on frame-rate dependency of RBC velocity. 第33回日本微小循環学会総会、口演（平成20年2月東京）

6. Tatarishvili J, Tomita M, Tomita Y, Osada T, Unekawa M, Toriumi H, Suzuki N: A new "Y-Type" precortical arteriolo-arteriolar microanastomosis in the microvascular network of MCA. 第33回日本微小循環学会総会、口演（平成20年2月東京）

（国際学会）

1. Tomita Y, Tomita M, Osada T, Unekawa M, Toriumi H, Mihara B, Suzuki N: IN VIVO STAINING OF ASTROCYTIC ELEMENTS SURROUNDING MICROVESSELS WITH FLOWING RBCS IN MICE : Brain07, The 23rd International Symposium on Cerebral Blood Flow, Metabolism & Function, ポスター (May 2007; Osaka)

2. Unekawa M, Tomita M, Tomita Y, Osada T, Toriumi H, Suzuki N: EXTRAORDINARY HIGH FLOW CAPILLARIES IN THE CEREBRAL MICROVASCULAR NETWORK : Brain07, The 23rd International Symposium on Cerebral Blood Flow, Metabolism & Function, ポスター (May 2007; Osaka)

3. Osada T, Tomita M, Tomita Y, Unekawa M, Toriumi H, Suzuki N: RBC EXCLUSION WITHOUT CAPILLARY DIAMETRIC CHANGE

DURING PASSAGE OF K+-INDUCED CORTICAL SPREADING DEPRESSION IN RATS : Brain07, The 23rd International Symposium on Cerebral Blood Flow, Metabolism & Function, 口演 (May 2007; Osaka)

G．知的財産権の出願。登録状況（予定を含む）

該当なし

別添 5

表　研究成果の刊行に関する一覧表

刊行書籍又は雑誌名（雑誌のときは雑誌名、巻号数、論文名）	刊行年月日	刊行書店名	執筆者名
Feasibility study of a direct endo-aortic clamp balloon. *ASAIO J.* 2007;53:136-9.	2007 年 4 月	Lippincott Williams & Wilkins	Anzai T, Iino Y, Kumeno T, Yozu R.
'Working' cardiomyocytes exhibiting plateau action potentials from human placenta-derived extraembryonic mesodermal cells. *Exp. Cell Res.* 313, 2550-62 (2007).	2007 年 7 月	Elsevier	Okamoto K, Miyoshi S, Toyoda M, Hida N, Ikegami Y, Makino H, Nishiyama N, Tsuji H, Cui CH, Segawa K, Uyama T, Kami D, Miyado K, Asada H, Matsumoto K, Saito H, Yoshimura Y, Ogawa S, Aeba R, Yozu R, Umezawa A.
Administration of granulocyte colony-stimulating factor after myocardial infarction enhances the recruitment of hematopoietic stem cell-derived myofibroblasts and contributes to cardiac repair. *Stem Cells.* 2007;25:2750-9	2007 年 11 月	AlphaMed Press	Fujita J, Mori M, Kawada H, Ieda Y, Tsuma M, Matsuzaki Y, Kawaguchi H, Yagi T, Yuasa S, Endo J, Hotta T, Ogawa S, Okano H, Yozu R, Ando K, Fukuda K.
Use of an epidural cooling catheter with a closed countercurrent lumen to protect against ischemic spinal cord injury in pigs. *J Thorac Cardiovasc Surg.* 2007 ;134:1220-6.	2007 年 11 月	Elsevier	Yoshitake A, Mori A, Shimizu H, Ueda T, Kabei N, Hachiya T, Okano H, Yozu R.
[Safety measures of extracorporeal circulation by heart surgeons and perfusionists] *Kyobu Geka.* 2007 ;60:1055-9. Japanese.	2007 年 11 月	南江堂	Tomizawa Y, Momose N, Matayoshi T, Yozu R, Takamoto S.
Stress distribution on the thorax after the Nuss procedure for pectus excavatum results in different patterns between adult and child patients. *J Thorac Cardiovasc Surg.* 2007;134:1502-7.	2007 年 12 月	Elsevier	Nagasao T, Miyamoto J, Tamaki T, Ichihara K, Jiang H, Taguchi T, Yozu R, Nakajima T.
Aortic translocation with autologous tissue. *Tex. Heart Inst. J.* 34, 420-2 (2007).	2007 年 12 月	Texas Heart Institute	Aeba R, Yozu R.
A case report of surgical correction for congenital mitral regurgitation with subvalvular apparatus abnormality. *Gen. Thorac. Cardiovasc. Surg.* 56, 36-8 (2008).	2008 年 1 月	Springer	Kudo M, Yozu R, Aeba R, Kokaji K, Kimura N, Iwanaga S.

刊行書籍又は雑誌名（雑誌のときは雑誌名、巻号数、論文名）	刊行年月日	刊行書店名	執筆者名
Blatchford scoring system is a useful scoring system for detecting patients with upper gastrointestinal bleeding who do not need endoscopic intervention. *J. Gastroenterol. Hepatol.* 22, 1404-8 (2007).	2007 年 9 月	Blackwell Publishing	Masaoka T, Suzuki H, Hori S, Aikawa N, Hibi T.
Application of the recent american practice resources for risk stratification system for patients presenting to a Japanese emergency department because ofsyncope. *Int. Heart J.* 48, 513-22 (2007).	2007 年 7 月	International Heart Journal Association	Suzuki M, Hori S, Aikawa N.
The Incidence of sickness/trauma in spectators of professional baseball at the Meiji Jingu Baseball Stadium. *Keio J. Med.* 56, 85-91 (2007).	2007 年 9 月	慶應医学会	Ishikawa H, Hori S, Aikawa N.
Prostaglandin E2 induces hypertrophic changes and suppresses alpha-skeletal actin gene expression in rat cardiomyocytes. *J. Cardiovasc. Pharmacol.* 50, 548-54 (2007).	2007 年 11 月	Lippincott Williams & Wilkins	Miyatake S, Manabe-Kawaguchi H, Watanabe K, Hori S, Aikawa N, Fukuda K.
Adenosine triphosphate-sensitie potassium channels prevent extension of myocardial ischemia to subepicardium during hemorrhagic shock. *Shock.*	2008 年 (印刷中)	Lippincott Williams & Wilkins	Nakagawa M, Hori S, Adachi T, Miyazaki K, Inoue S, Suzuki M, Mori H, Nakazawa H, Aikawa N, Ogawa S.
meso-Tetrakis(α , α , α , α -o-amidophenyl) porphinatoiron(II) bearing a proximal histidyl group at the β -pyrrolic position via an acyl bond: synthesis and O_2 coordination in aqueous media. *Chem. Lett.* 36. 640–641 (2007).	2007 年 5 月	日本化学会	A. Nakagawa, T. Komatsu, E. Tsuchida.
Influence of O_2-carrying plasma hemoprotein "albumin-heme" on complement system and platelet activation in vitro and physiological responses to exchange transfusion. *J. Biomed. Mater. Res. 81A*, 821–826 (2007)	2007 年 6 月	Wiley	T. Komatsu, Y. Huang, S. Wakamoto, H. Abe, M. Fujihara, H. Azuma, H. Ikeda, H. Yamamoto, H. Horinouchi, K. Kobayashi, E. Tsuchida.
Induced long-range attractive potentials of human serum albumin by ligand binding. *Phys. Rev. Lett. 98*, 208101-1–4 (2007).	2007 年 5 月	The American Physical Society	T. Sato, T. Komatsu, A. Nakagawa, E. Tsuchida.
O_2-binding albumin thin films: solid membranes of poly(ethylene glycol)-conjugated human serum albumin incorporating iron porphyrin. *Bioconjugate Chem. 18*, 1673–1677 (2007).	2007 年 9 月	American Chemical Society	A. Nakagawa, T. Komatsu, Y. Huang, G. Lu, E. Tsuchida.

刊行書籍又は雑誌名（雑誌のときは雑誌名、巻号数、論文名）	刊行年月日	刊行書店名	執筆者名
Genetic engineering of the heme pocket in human serum albumin: modulation of O_2 binding of iron protoporphyrin IX by variation of distal amino acids. *J. Am. Chem. Soc. 129*, 11286–11295 (2007).	2007 年 9 月	American Chemical Society	T. Komatsu, A. Nakagawa, P. A. Zunszain, S. Curry, E. Tsuchida.
Heme pocket architecture in human serum albumin: regulation of O_2 binding affinity of a prosthetic heme group by site-directed mutagenesis. *Macromol. Symp.* (in press).	2008 年 (印刷中)	Wiley	T. Komatsu, A. Nakagawa, E. Tsuchida.
O_2 binding to human serum albumin incorporating iron porphyrin with a covalently linked methyl-L-histidine isomer. *Bioconjugate Chem.* (in press).	2008 年 (印刷中)	American Chemical Society	A. Nakagawa, T. Komatsu, M. Iizuka, E. Tsuchida.
Systemic administration of hemoglobin vesicles elevates tumor tissue oxygen tension and modifies tumor response to irradiation. *J. Surg. Res.*	In press	Elsevier	M. Yamamoto, Y. Izumi, H. Horinouchi, Y. Teramura, H. Sakai, M. Kohno, M. Watanabe, T. Adachi, E. Ikeda, S. Takeoka, E. Tsuchida, K. Kobayashi.
Hemoglobin-vesicles as artificial oxygen carriers: Present situation and future vision. *J. Intern. Med.* 263, 4-15 (2008).	2008 年 1 月	Blackwell Publishing Co.	H. Sakai, K. Sou, H. Horinouchi, K. Kobayashi, E. Tsuchida.
Effects of hemoglobin vesicles, a liposomal artificial oxygen carrier, on hematological responses, complement and anaphylactic reactions in rats. *Artif. Cells Blood Substitutes Biotechnol.* 35, 157-172 (2007).	2007 年 3 月	Informa Healthcare	H. Abe, H. Azuma, M. Yamaguchi, M. Fujihara, H. Sakai, S. Takeoka, E. Tsuchida, H. Ikeda.
Effects of hemoglobin vesicles, a cellular-type artificial oxygen carrier, on human hematopoietic stem/progenitor cells in vitro. *J. Biomed. Materials Res. A.* (in press).	2008 年 (印刷中)	Wiley	M. Yamaguchi, M. Fujihara, S. Wakamoto, H. Sakai, S. Takeoka, E. Tsuchida, H. Hamada, H. Azuma, H. Ikeda.
Selective uptake of surface-modified phospholipid vesicles by bone marrow macrophages in vivo. *Biomaterials* 28, 2655-66 (2007).	2007 年 6 月	Elsevier	K. Sou, B. Goins, S. Takeoka, E. Tsuchida, W.T. Phillips
Rheological properties of hemoglobin vesicles (artificial oxygen carriers) suspended in a series of plasma substitute solutions. *Langmuir* 23, 8121-8128 (2007).	2007 年 6 月	American Chemical Society	H. Sakai, A. Sato, S. Takeoka, E. Tsuchida.

刊行書籍又は雑誌名（雑誌のときは雑誌名、巻号数、論文名）	刊行年月日	刊行書店名	執筆者名
Encapsulation of concentrated hemoglobin solution in phospholipid vesicles retards the reaction with NO, but not CO, by intracellular diffusion barrier. *J. Biol. Chem.* 283, 1508-1517 (2008)	2008 年 1 月	The American Society for Biochemistry and Molecular Biology, Inc.	H. Sakai, A. Sato, K. Masuda, S. Takeoka, E. Tsuchida.
Electrostatic interactions and complement activation on the surface of phospholipid vesicle containing acidic lipids: Effect of the structure of acidic groups. *Biochim Biophys Acta.* (in press).	2008 年 (印刷中)	Elsevier	K. Sou, E. Tsuchida.
各種代用血漿剤に分散させたヘモグロビン小胞体（人工赤血球）とその血液混合系のレオロジー特性. *日本ヘモレオロジー学会誌* (in press)	2008 年 (印刷中)	日本ヘモレオロジー学会	佐藤 敦、酒井 宏水、武岡 真司、土田 英俊.
NO and CO binding profiles of hemoglobin vesicles as artificial oxygen carriers. *Biochim Biophys Acta.* (in press).	2008 年 (印刷中)	Elsevier	H. Sakai, A. Sato, P. Sobolewski, S. Takeoka, J.A. Frangos, K. Kobayashi, M. Intaglietta, E. Tsuchida.
Hemoglobn vesicles to treat hypoxia in critically ischemic tissue. *Artif. Blood* 15, 58-64 (2007).	2007 年 12 月	日本血液代替物学会	D. Erni, R. Wettstein, C. Contaldo, J. Plock, N. Rafatmehr, H. Sakai, E. Tsuchida.
輸血の代替が可能な酸素輸液の実現と組織再生技術. *環境と健康* 20, 464-472 (2007)	2007 年 12 月	共和書院	酒井宏水、土田英俊.
Hemoglobin-vesicles for a Transfusion Alternative and Targeted Oxygen Delivery. *J. Liposome Res.* 17, 227- 235 (2007).	2007 年 7 月	Informa Healthcare USA, Inc.	H. Sakai, E. Tsuchida.
Solution to the problems of acellular Hbs by encapsulation, and the intrinsic issues of Hb-vesicles as a molecular assembly. *Transfusion Alternatives in Transfusion Medicine* 9, 226-236 (2007).	2007 年 12 月	Blackwell Publising	H. Sakai, K. Sou, E. Tsuchida.
人工赤血球(HbV)と酸素運搬機能および組織酸素代謝. 至適 Hb レベルならびに人工赤血球の展望. *体液・代謝管理* 23, 35-42 (2007).	2007 年	体液・代謝管理研究会	杖下隆哉、寺嶋克幸、坂本篤裕.

刊行書籍又は雑誌名（雑誌のときは雑誌名、巻号数、論文名）	刊行年月日	刊行書店名	執筆者名
A Matrix Metalloproteinase Inhibitor, ONO-4817, Suppresses the Development of Aortic Intimal Hyperplasia in Experimental Hyperlipidemic Rabbit. *Int. Heart J.* 48,369-378 (2007)	2007年5月	International Heart Journal Association	Y. Okamoto, K. Satomura, K. Nakaya, N. Tanaka, F. Ohsuzu, J. Imaki, M. Yoshioka, H. Nakamura.
Telmisartan Enhances Cholesterol Efflux from THP-1 Macrophages by Activating PPARgamma. *J. Atheroscler. Thromb.* 14, 133-141 (2007).	2007年6月	Japan Atherosclerosis Society	K. Nakaya, M. Ayaori, T. Hisada, S. Sawada , N. Tanaka, N. Iwamoto, M. Ogura, E. Yakushiji , M. Kusuhara, H. Nakamura, F. Ohsuzu.
Large Right Coronary Artery to Left Ventricle Fistula. *J. Echocardiography* 5, 58-60 (2007)	2007年9月	Japanese Society of Echocardio-graphy	N. Tanaka, K. Isoda, M. Hara, K. Hayashi, K. Miyazaki, K. Kimura, K. Arakawa, M. Kusuhara , F. Ohsuzu.
Magnetic Resonance Evaluation of the Associatins of Thoracic and Abdominal Aortic Plaques with the Presence and Extent of Coronary Artery Stenosis. *J. Cardiovasc. Magnetic Resonance* 9, 855-861 (2007)	2007年11月	Informa Healthcare USA Inc.	K. Ashida, Y. Momiyama, Zahi A.Fayad, N. Tanaka, R. Kato, H. Taniguchi, R. Ohmori, T. Kihara, A. Kameyama, M. Nagata, H. Nakamura, F. Ohsuzu.
Effect of hemoglobin vesicle, a cellular-type artificial oxygen carrier, on middle cerebral artery occlusion- and arachidonic acid-induced stroke models in rats. *Neurosci. Lett.* 421, 121-125 (2007).	2007年6月	Elsevier	H. Komatsu, T. Furuya, N. Sato, K. Ohta, A. Matsuura, T. Ohmura, S. Takagi, M. Matsuura, M. Yamashita, M. Itoda, J. Itoh, H. Horinouchi, K. Kobayashi.
救急医療の現場での輸血医療の実態と人工酸素運搬体への期待. *救急医学* 31, 981-986 (2007)	2007年8月	へるす出版	高折益彦、堀之内宏久、小林紘一
Syndrome of inappropriate secretion of antidiuretic hormone after chemotherapy with vinorelbine. *Cancer Chemother. Pharmacol.*	2008年 (印刷中)	Springer	H. Kuroda, M. Kawamura, T. Hato, K. Kamiya, M. Kawakubo, Y. Izumi, M. Watanabe, H. Horinouchi, K. Kobayashi.
Sampling rate-dependent RBC velocity in intraparenchymal single capillaries of rat cerebral cortex. *Microvasc. Rev. Commun.* 1, 12-15 (2007).	2007年4月	日本微小循環学会	Unekawa M, Tomita M, Osada T, Tomita Y, Toriumi H, Suzuki N.

刊行書籍又は雑誌名（雑誌のときは雑誌名、巻号数、論文名）	刊行年月日	刊行書店名	執筆者名
Automated method for tracking vast numbers of FITC-labeled RBCs in microvessels of rat brain in vivo using a high-speed confocal microscope System. Microcirculation 15, 163-174 (2008)	2008年2月	Informa Healthcare USA Inc.	Tomita M, Osada T, Istvan S, Tomita Y, Unekawa M, Toriumi H, Tanahashi N, Suzuki N.
Nitric oxide vanished capillary RBC in the face of an increase in arteriolar flow in the rat cerebral cortex. *Microvasc. Rev. Commun.*, in press.	2008年 (印刷中)	日本微小循環学会	Tomita M, Osada T, Unekawa M, Tomita Y, Toriumi H, Suzuki N.

その他刊行物

1. 日本血液代替物学会、早大、血液由来のヘモグロビンを使わない次世代人工酸素運搬体を提案. 日経バイオテク 2007年6月15日

2. Newton Highlight (ニュートン コリア) 2006年にニュートン誌に掲載された人工赤血球の記事が韓国版にも掲載された。2008年1月15日

研究成果の刊行物・別冊

(2007. 4. ～ 2008. 3.)

Feasibility Study of a Direct Endo-Aortic Clamp Balloon

TOMOHIRO ANZAI,* YOSHIMI IINO,* TAKASHI KUMENO,† AND RYOHEI YOZU*

We have developed a new end-aortic clamp balloon catheter intended to be inserted directly into, thereby occluding, the ascending aorta. We examined the performance of this catheter in a canine model. We evaluated the extent of migration tolerance of the catheter under cardiopulmonary bypass perfusion in 12 mongrel dogs, weighing 20 kg, under general anesthesia. After institution of cardiopulmonary bypass, this catheter was inserted into the ascending aorta, and the balloon was inflated to occlude the ascending aorta. After the canine heart was arrested following the administration of cardioplegic solution, balloon migration was examined over a period of 3 hours, with hourly increases in perfusion pressure from 50 mm Hg to 80 mm Hg and finally to 100 mm Hg. After the migration test, ascending aortic wall sections, where the balloon was inflated, were examined microscopically. At internal balloon pressure of 300 to 400 mm Hg, migration occurred at perfusion pressure of ≥90 to 100 mm Hg. No histological differences were observed with use of the balloon catheter, compared with an extra-aortic clamp forceps. Based on these results, this device is safe, feasible, and can adequately occlude the ascending aorta during cardiopulmonary bypass. We conclude that this device is effective in patients weighing 20 kg. *ASAIO Journal* 2007; 53:136–139.

Minimally invasive cardiac surgery (MICS) has been used as an alternative approach to conventional cardiac surgery since 1995,[1,2] with an equivalent outcome, but it is less invasive and requires a smaller incision. Various technologies for use in MICS have improved the effectiveness of the surgery.[3–7] These include devices to enhance extracorporeal circulation and facilitate aortic clamping,[8] a maneuver that is essential for intracardiac repair during surgery.

Clamping of the ascending aorta in median full sternotomy is straightforward, but this procedure is much more difficult to perform safely from a small incision in MICS. In particular, the Port-Access System (Cardiovations, Ethicon Inc, Somerville, NJ), in which the endo-aortic clamp (EAC) balloon catheter is inserted in retrograde fashion from the peripheral artery, is difficult to use in Japanese patients of small stature.[9] For this reason, we have developed a balloon catheter, which we refer to as a direct EAC balloon, that can be directly inserted into the ascending aorta. The device is composed of a three-lumina catheter including one balloon made of medical grade polypropylene[10] and two other lumina catheters, the cardioplegia port and the vent lumen port. We also developed a half-size model of the balloon catheter in the same fashion for experimental use. This EAC balloon catheter has two lumina, one for the balloon, which is made of wire-reinforced polypropylene. The other lumina, for the infusion port, was selected from 13 kinds of polypropylene material, based on compliance and durability. We tested the isolated dog aorta under pressures of 50 mm Hg, 80 mm Hg, and 100 mm Hg every hour for a of total 3 hours. We developed the geometry of the catheter and evaluated the ability of the new balloon to occlude the aorta.

In this study, we examined the extent of the migration tolerance of our newly designed catheter in a canine model.

Materials and Methods

The newly designed balloon catheter was intended to allow insertion directly into the ascending aorta, in contrast to the commercially available port-access system, in which the catheter is inserted through the peripheral vasculature. The direct EAC balloon catheter has the following advantages: inflation of the device is possible within the ascending aorta to occlude the lumen and thus to stop blood flow; the balloon can be secured without any risk of migration; the device allows injection of cardioplegic solution through the catheter; the device is easy to insert and safe to use; the narrow catheter in the device reduces disturbance of the operative field; and, the device can be used in versatile ways in almost all cardiac procedures.

The configuration of the balloon catheter is shown in **Figure 1**. The catheter is 40 cm in length and the outer diameter is 3.6 mm (12F). The mold size of the balloon is 20 mm in diameter, with the maximum inflated size being 80 mm in diameter. We also developed a half-size model of the balloon catheter in the same fashion for experimental use. This EAC balloon catheter is 30 cm in length, with outer diameter of 2.0 mm (**Figure 2**). The balloon size and the capacity of the catheter is half the size of the original device.

The method used in the study involved performing cardiopulmonary bypass (CPB) with the balloon in 12 mongrel dogs (20 kg) under general anesthesia. First, ketamine hydrochloride (25 mg/kg) was administered intravenously, and anesthesia was maintained with intravenous pentobarbital and inhaled isoflurane. All dogs were mechanically ventilated with 100% oxygen through an endotracheal tube.[11] For monitoring during surgery, an electrocardiogram, rectal temperature, artery pressure of the carotid artery, balloon internal pressure, aortic root pressure, and perfusion pressure were recorded (**Figure 3**).

A right thoracotomy was performed at the fifth intercostal space, and the location of the ascending aorta was confirmed and outer diameter was measured. Heparin sulfate (60 U/kg)

From the *Department of Cardiovascular Surgery, School of Medicine, Keio University, and †Office of Technology Transfer, Japan Science and Technology Corporation, Tokyo, Japan.

Submitted for consideration March 2006; accepted for publication in revised form September 2006.

Reprint Requests: Dr. Tomohiro Anzai, The Division of Cardiovascular Surgery, Keio University, 35 Shinanomachi, Shinjuku, Tokyo 160-8582, Japan; E-mail: anzai221@aol.com.

DOI: 10.1097/MAT.0b013e31802e1dc9

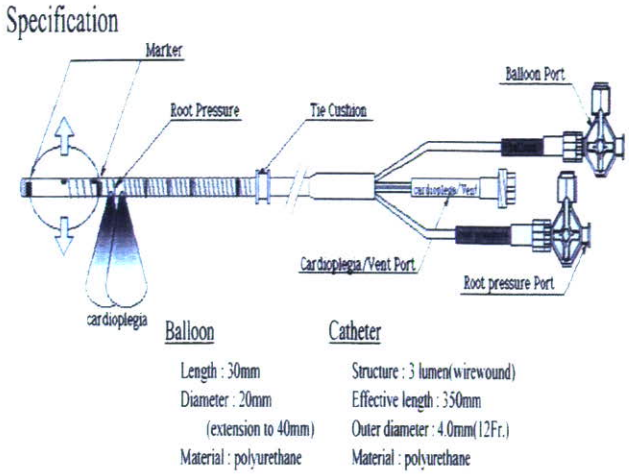

Figure 1. Direct endo-aortic clamp (EAC) balloon.

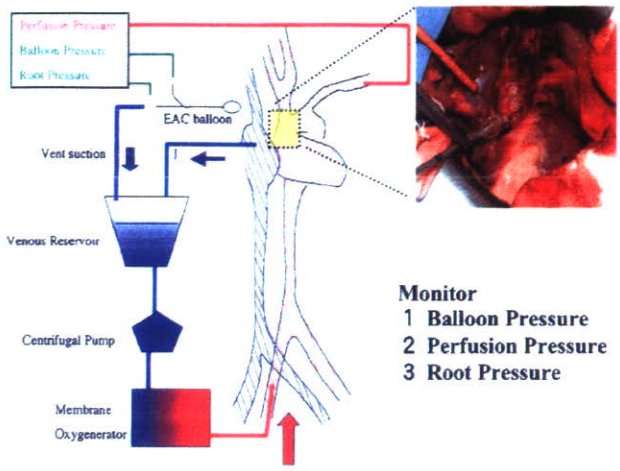

Figure 3. Animal model. For monitoring during surgery, an electrocardiogram, rectal temperature, artery pressure of the carotid artery, balloon internal pressure, aortic root pressure, and perfusion pressure were recorded.

was injected intravenously. The rectal temperature was kept at 30°C during CPB. We cannulated into the right femoral artery and the right atrium with a two-stage cannula; an aortic root cannula was inserted into the ascending aorta and kept in during the procedure. The EAC balloon catheter was inserted into the ascending aorta by the Seldinger method and positioned while systemic arterial pressure and aortic root pressure were noted. The balloon was then inflated, with confirmation that the internal pressure of the balloon was 300 to 400 mm Hg, and a cardioplegic solution (10 mL/kg) was injected. Migration of the balloon was estimated while increasing the perfusion pressure hourly from 50 mm Hg to 80 mm Hg and finally to 100 mm Hg, over a total of 3 hours. In addition, the same experiment was performed by using the extra-aortic clamp forceps (EACF) method, and the histology of the region adjacent to the fixed part of the direct EAC balloon catheter was compared with a similar region following use of the EACF method.

Results

In all dogs, the EAC balloon catheter was inserted into the best position; it was achieved with the surgeon looking directly at the aorta and monitoring the blood pressure. At a balloon pressure of 300 to 400 mm Hg, the EAC balloon did not migrate into the ascending aorta at systemic perfusion pressures up to 100 mm Hg (**Figure 4**). However, when the pump pressure exceeded 100 mm Hg, migration of the balloon occurred, suggesting that this is the pressure threshold of the EAC balloon catheter (**Figure 5**).

A histological evaluation using hematoxylin and eosin staining and elastic fiber staining was performed. Few histological differences were observed between animals treated using the EAC balloon and those treated using EACF. In the EACF method, most of the arterial wall at the clamp position showed normal histology; however, changes were seen in some areas. Most endothelial cells were detached, some intima were mildly degenerated and necrotic, and some smooth muscle cells of the media were necrotic (**Figure 6**); these changes are thought to result from compression by the aortic clamp forceps. In the EAC method, the arterial wall at the clamp position also mainly demonstrated normal histology; however, changes were seen in some areas. The connective tissue of the media had loosened, but none of the smooth muscle cells of the

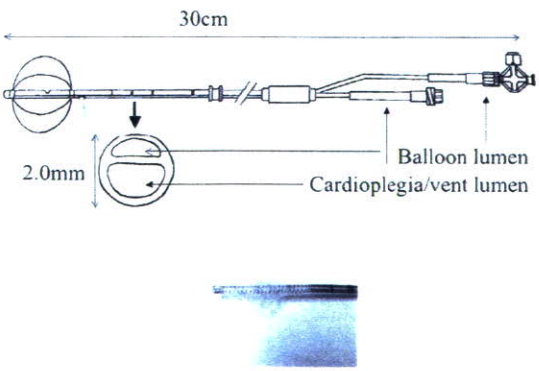

Figure 2. Direct EAC balloon (animal-sized model).

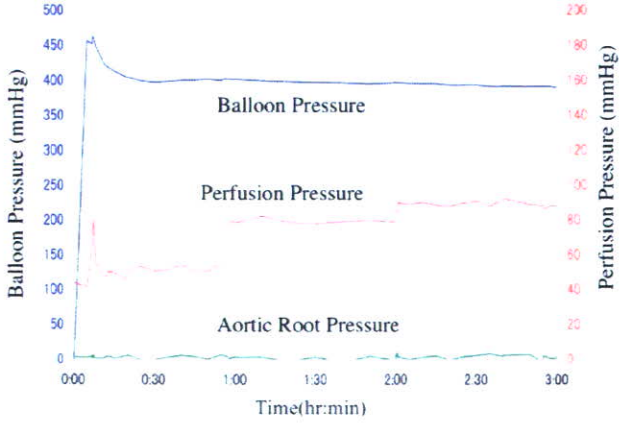

Figure 4. Pressure-time curve. At a balloon pressure of 300 to 400 mm Hg, the EAC balloon did not migrate into the ascending aorta for systemic perfusion pressures up to 100 mm Hg.

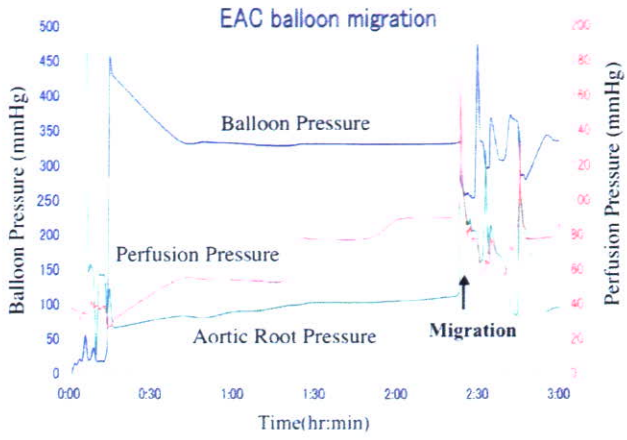

Figure 5. Migration resistance threshold. When the pump pressure exceeded 100 mm Hg, migration of the balloon occurred.

media were necrotic. However, some endothelial cells had become detached and necrotic changes in these cells were observed (**Figure 7**). These histological changes are thought to result from compression by the EAC balloon from the interior of the aorta.

Discussion

Minimally invasive cardiac surgery is likely to be one of the main approaches to cardiac surgery in the future. Given this, a device that allows aortic occlusion through a small incision is necessary, such that this surgery can be performed as effectively as with median sternotomy.[12,13] Aortic clamping is an important aspect of MICS, and confirmation of the stability of the EAC balloon at normal blood pressure is required before its use in aortic clamping in cardiac surgery.

Conventionally, aortic clamping has used an approach from the femoral artery, based on the port-access system. However,

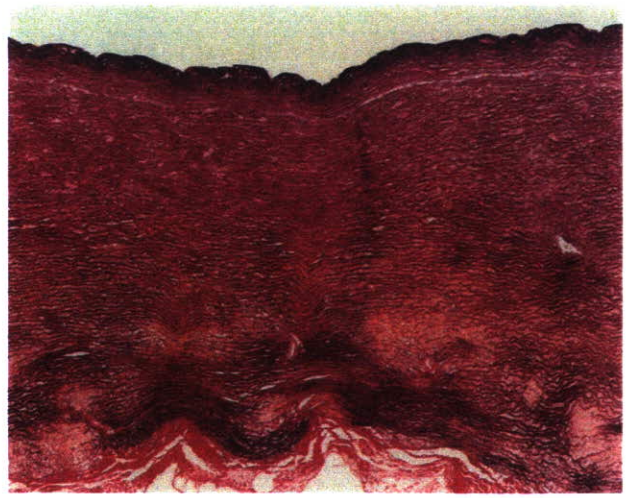

Figure 6. Elastic fiber stain of extra-aortic clamp forceps (EACF). Most endothelial cells were detached; some intima were mildly degenerate and necrotic; some smooth muscle cells of the media were necrotic.

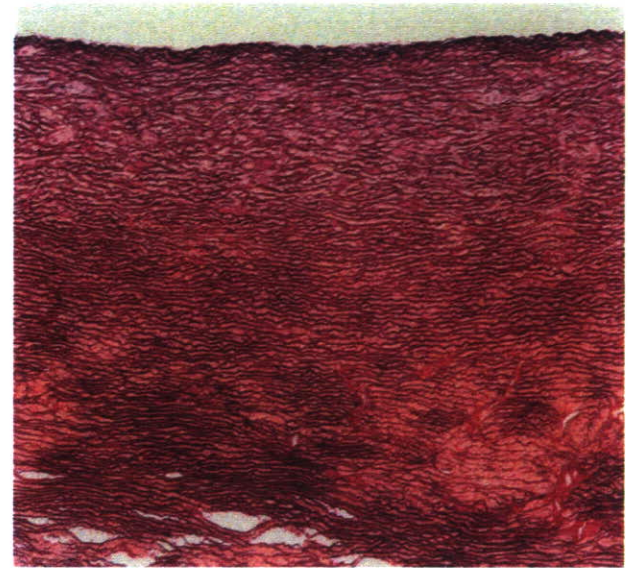

Figure 7. Elastic fiber stain of endo-aortic clamp balloon (EACB). The connective tissue of the media had loosened, but none of the smooth muscle cells of the media were necrotic. Some endothelial cells had become detached, and necrotic changes in these cells were observed.

this device can lead to arteriovenous complications in the lower extremities as the result of migration, and it is also difficult to use the device in Japanese patients of small stature. In contrast, our new aortic clamping device, the so-called EAC balloon catheter, is not restricted in this way, since it allows direct insertion from the ascending aorta. In the current study, the device was able to resist a pressure of about three times that of normal blood pressure, suggesting that application of the EAC balloon catheter in clinical practice should be possible.

As an example of the use of the EAC balloon catheter, we describe the case of an atrial septal defect leading to cardiac arrest, in which the extent of inflation of the EAC balloon was measured by using the ascending aorta diameter determined by CT in the patient, since the inflation-volume curve and the balloon diameter are related. The EAC balloon catheter was inserted from some distance away, and surgery was completed without disturbing the intracardiac conditions. This led to a good outcome, and the patient was discharged from hospital on the third postoperative day. Specific assessment of the EAC balloon catheter in the future will require evaluation of its stability and other properties of the balloon catheter in an arteriosclerosis model. However, the stability of the half-sized model developed in the current study suggests that this device may be applicable to cardiac surgery in children weighing up to 20 kg without arteriosclerosis.

Conclusion

In conclusion, we have developed a new direct endo-aortic occlusion balloon catheter for technological support of the MICS procedure and shown that it can be easily and safely used without use of a fluoroscopy. The results show that the EAC balloon catheter can occlude the ascending aorta during CPB, and the balloon shows sufficient stability to suggest that

it would be tolerant in clinical use. In addition, the direct EAC balloon catheter has potential for use in reoperation without adhesiotomy, and the half-size model of the direct EAC balloon catheter has potential for use in children weighing up to 20 kg.

References

1. Benneti FJ, Ballester C, Sani G, *et al*: Video-assisted coronary bypass surgery. *J Card Surg* 10: 620–625, 1995.
2. Schwartz DS, Ribakove GH, Grossi EA, *et al*: Minimally invasive cardiopulmonary bypass with cardioplegic arrest: a closed chest technique with equivalent myocardial protection. *J Thorac Cardiovasc Surg* 111: 556–566, 1996.
3. Chitowood WR Jr, Nifong LW, Chapman WH, *et al*: Robotic surgical training in an academic institution. *Ann Surg* 234: 475–484, 2001; discussion 234: 484–486, 2001.
4. Mohr FW, Falk V, Diegeler A, *et al*: Computer-enhanced 'robotic' cardiac surgery: experience in 148 patients. *J Thorac Cardiovasc Surg* 121: 842–853, 2001.
5. Chitowood WR Jr, Elbeery JR, Moran JF, *et al*: Minimally invasive mitral valve repair using transthoracic aortic occlusion. *Ann Surg* 63: 1477–1479, 1997.
6. Chitowood WR Jr, Elbeery JR, Chapman WH, *et al*: Video-assisted minimally invasive mitral valve surgery: the 'micro-mitral' operation. *Thorac Cardiovasc Surg* 113: 413–414, 1997.
7. Schneider F, Falk V, Walther T, Mohr FW: Control of endoaortic clamp position during port-access mitral valve operations using transcranial Doppler echography. *Ann Thorac Surg* 65: 1481–1482, 1998.
8. Fann JI, Pompili MF, Stevens JH, *et al*: Port-access cardiac operations with cardioplegic arrest. *Ann Thorac Surg* 63: S35–S39, 1997.
9. Wimmer-Greinecker G, Matheis G, Dogan S, *et al*: Complications of port-access cardiac surgery. *J Card Surg* 14: 240–245, 1999.
10. Yozu R, Shin H, Mitsumaru A, *et al*: A new endo-aortic occlusion balloon: the 'Direct Endo-Aortic Clamp (EAC) balloon'. *ASAIO J* 47: 254–256, 2001.
11. Pompili MF, Stevens JH, Burdon TA, *et al*: Port access mitral valve replacement in dogs. *J Thorac Cardiovasc Surg* 112: 1268–1274, 1996.
12. Yozu R, Kawada S: Minimally invasive cardiac surgery, in Arai T (ed), *Surgery for Heart Valve Disease*, Tokyo, Igakushoin, pp. 383–394, 1998.
13. Yozu R, Shin H, Maehara T: Minimally invasive cardiac surgery (MICS) for valvular disease; in Omoto R (Ed), *Minimally Invasive Cardiac Surgery*, Tokyo, Shindan to Chiryosha, pp. 95–105, 1999.

EXPERIMENTAL CELL RESEARCH 313 (2007) 2550–2562

available at www.sciencedirect.com

ScienceDirect

www.elsevier.com/locate/yexcr

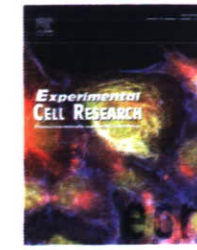

Research Article

'Working' cardiomyocytes exhibiting plateau action potentials from human placenta-derived extraembryonic mesodermal cells

Kazuma Okamoto[a,b], *Shunichiro Miyoshi*[c,d], *Masashi Toyoda*[a], *Naoko Hida*[a,c], *Yukinori Ikegami*[c], *Hatsune Makino*[a], *Nobuhiro Nishiyama*[c], *Hiroko Tsuji*[a,f], *Chang-Hao Cui*[a], *Kaoru Segawa*[e], *Taro Uyama*[a], *Daisuke Kami*[a], *Kenji Miyado*[a], *Hironori Asada*[f], *Kenji Matsumoto*[g], *Hirohisa Saito*[g], *Yasunori Yoshimura*[f], *Satoshi Ogawa*[c], *Ryo Aeba*[b], *Ryohei Yozu*[b], *Akihiro Umezawa*[a,*]

[a]*Department of Reproductive Biology and Pathology, National Research Institute for Child Health and Development, Tokyo, Japan*
[b]*Department of Surgery, Keio University School of Medicine, Tokyo, Japan*
[c]*Cardio-pulmonary Division of Keio University School of Medicine, Tokyo, Japan*
[d]*Institute for Advanced Cardiac Therapeutics, Keio University School of Medicine, Tokyo, Japan*
[e]*Department of Microbiology and Immunology, Keio University School of Medicine, Tokyo, Japan*
[f]*Department of Obstetrics and Gynecology, Keio University School of Medicine, Tokyo, Japan*
[g]*Department of Allergy and Immunology, National Research Institute for Child Health and Development, Tokyo, Japan*

ARTICLE INFORMATION

Article Chronology:
Received 24 August 2006
Revised version received
19 April 2007
Accepted 24 April 2007
Available online 5 May 2007

Keywords:
Placenta
Co-culture
Cardiac differentiation

ABSTRACT

The clinical application of cell transplantation for severe heart failure is a promising strategy to improve impaired cardiac function. Recently, an array of cell types, including bone marrow cells, endothelial progenitors, mesenchymal stem cells, resident cardiac stem cells, and embryonic stem cells, have become important candidates for cell sources for cardiac repair. In the present study, we focused on the placenta as a cell source. Cells from the chorionic plate in the fetal portion of the human placenta were obtained after delivery by the primary culture method, and the cells generated in this study had the Y sex chromosome, indicating that the cells were derived from the fetus. The cells potentially expressed 'working' cardiomyocyte-specific genes such as cardiac myosin heavy chain 7β, atrial myosin light chain, cardiac α-actin by gene chip analysis, and Csx/Nkx2.5, GATA4 by RT-PCR, cardiac troponin-I and connexin 43 by immunohistochemistry. These cells were able to differentiate into cardiomyocytes. Cardiac troponin-I and connexin 43 displayed a discontinuous pattern of localization at intercellular contact sites after cardiomyogenic differentiation, suggesting that the chorionic mesoderm contained a large number of cells with cardiomyogenic potential. The cells began spontaneously beating 3 days after co-cultivation with murine fetal cardiomyocytes and the frequency of beating cells reached a maximum on day 10. The contraction of the cardiomyocytes was rhythmical and synchronous, suggesting the presence of electrical communication between the cells. Placenta-derived human fetal cells may be useful for patients who cannot supply bone marrow cells but want to receive stem cell-based cardiac therapy.

* *Corresponding author*. Fax: +81 3 5494 7048.
E-mail address: umezawa@1985.jukuin.keio.ac.jp (A. Umezawa).

0014-4827/$ – see front matter © 2007 Elsevier Inc. All rights reserved.
doi:10.1016/j.yexcr.2007.04.028

Introduction

Major advances have been made in the prevention, diagnosis, and treatment of ischemic heart disease and cardiomyopathy, including the use of heart transplantation and artificial hearts. However, the number of patients suffering from heart disease is still increasing [1]. Morbidity and mortality from cardiovascular diseases continue to be an enormous burden experienced by many individuals, with substantial economic cost. Enthusiasm for cell therapy for the injured heart has already reached the clinical setting, with physicians in several countries involved in clinical trials using several types of cell populations [2,3]. Bone-marrow-derived mononuclear cells [4,5], unfractioned bone marrow cells [6], bone-marrow-derived CD133$^+$ cells [7], and myoblasts [8] have been injected into the ischemic heart clinically.

Mesenchymal stem cells (MSCs) are a potential cellular source for stem cell-based therapy, since they have the ability to proliferate and differentiate into mesodermal tissues, including the heart tissue, and entail no ethical problems [9]. Human MSCs have been used clinically to treat patients with graft versus host disease and osteogenesis imperfecta [10,11]. We previously showed that murine and human marrow-derived MSCs can differentiate into cardiomyocytes and start to beat synchronously in vitro [12,13]. In addition, we and other groups proposed that direct injection of murine MSCs into the heart is a feasible approach in murine models of ischemic heart disease and in the normal mouse heart [14,15]. Although MSC transplantation slightly improved impaired cardiac function, this effect was limited. One of the reasons for this may be due to an extremely low rate of cardiomyogenesis from marrow-derived MSCs in vitro [13] and in vivo [14–17]. In order to further improve cardiac function, we have been searching for another source of MSCs having highly cardiomyogenic potential.

The placenta is composed of the amniotic membrane, chorionic mesoderm, and decidua; the amniotic membrane and chorionic mesoderm are the fetal portion and the decidua is the maternal portion (Fig. 1A) [18]. Recently it was reported that the chorionic villi of the placenta differentiated into osteocytes, chondrocytes and adipocytes under specific culture conditions [19,20]. In this study, we generated cells with the mesenchymal phenotype from the chorionic mesoderm, and

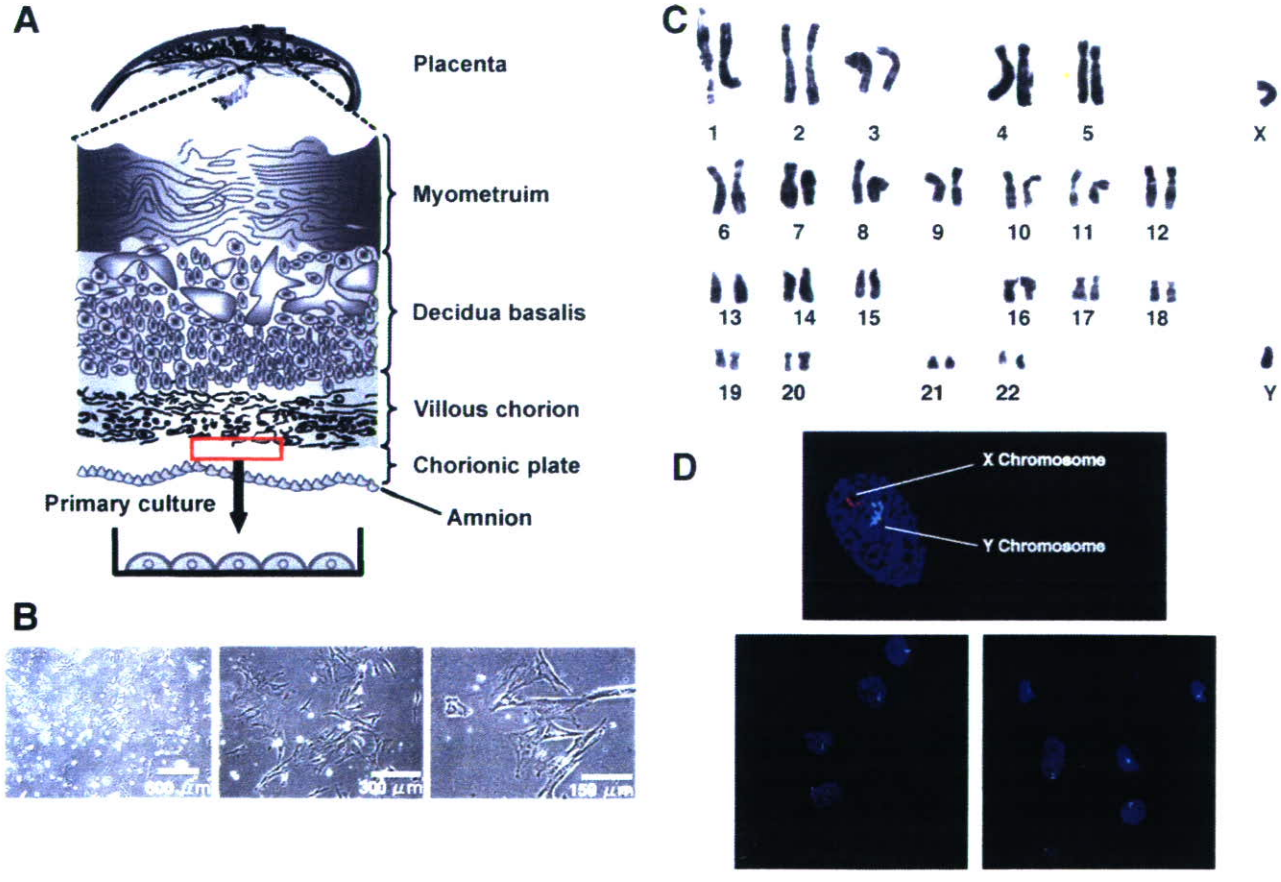

Fig. 1 – Establishment of chorionic plate cells. (A) Chorionic plate cells were established by primary culture of chorionic plate (red square in the chorionic mesoderm) in the human placenta. (B) Chorionic plate cells at PD 4 consisted of heterogeneous cell population. Three images show chorionic plate cells in the same culture dish. Their shape is different from that of fibroblasts. (C) Karyotyping by G-banding stain of chorionic plate cells. No chromosomal aberration was detected. (D) Chorionic plate cells have one X chromosome (red) and one Y chromosome (light blue). Nuclei were stained with DAPI (blue). (E) Flowcytometric analysis of chorionic plate cells using antibodies for CD14, CD29, CD31, CD34, CD44, CD45, CD59, CD73, CD90, CD105 and CD166. Black lines and shaded areas indicate reactivity of antibodies for isotype controls and that of antibodies for cell surface markers, respectively.

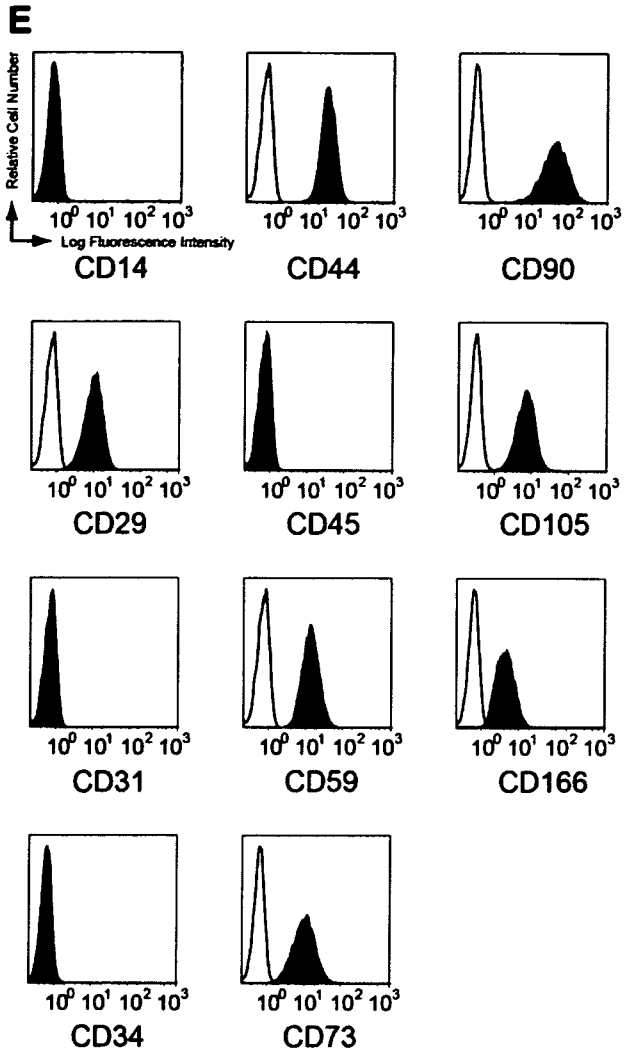

Fig. 1 (*continued*).

showed that: (a) physiologically functioning cardiomyocytes were transdifferentiated from human placenta-derived chorionic plate cells, but clear osteogenic and adipogenic phenotypes were not induced; (b) the cardiomyogenic induction rate obtained using our system was relatively high compared to that obtained using the previously described method [13]; (c) cocultivation with fetal murine cardiomyocytes alone without transdifferentiation factors such as 5-azaC or oxytocin is sufficient for cardiomyogenesis in our system; (d) chorionic plate cells have the electrophysiological properties of 'working' cardiomyocytes. The chorionic mesoderm contained a large number of cells with a cardiomyogenic potential.

Materials and methods

Chorionic plate cell culture

A human placenta was collected after delivery of a male neonate with informed consent. The study was approved by the ethics committee of Keio University, Tokyo, Japan (Number 17-44-1). To isolate chorionic plate cells, we used the explant culture method, in which the cells were outgrown from pieces of chorionic plate attached to dishes (Fig. 1A). Briefly, the decidua of the maternal part was separated and discarded. The chorionic plate from the fetal part were cut into pieces approximately 5 mm^3 in size. The pieces were washed in DMEM (high glucose; Kohjin Bio) supplemented with 100 U/ml penicillin–streptomycin (Gibco), 1 μg/ml Amphotericin B (Gibco) and 4 U/ml Novo-Heparin Injection 1000 (Mochidaseiyaku Co., Ltd.), until the supernatant was free of erythrocytes. Some pieces of chorionic plate were attached to the substratum in a 10-cm-diameter dish (Falcon, Becton, Dickinson and Company (BD), San Jose, CA, USA). Culture medium consisting of DMEM (high glucose; Kohjin Bio) supplemented with 10% FBS (CCT, Cansera, Canada) was added. The cells migrated out from the cut ends after approximately 20 days of incubation at 37 °C in 5% CO_2. The migrated cells were harvested with phosphate-buffered saline (PBS) with 0.1% trypsin and 0.25 mM EDTA (ethylenediamine-N,N,N',N'-tetraacetic acid) (Immuno-Biological Laboratories) for 5 min at 37 °C and counted. The harvested cells were re-seeded at a density of 3×10^5 cells in a 10-cm-diameter dish. Confluent monolayers of cells were subcultured at a 1:8 split ratio onto new 10-cm-diameter dishes and designated "chorionic plate cells". The culture medium was replaced with fresh culture medium every 3 or 4 days. The chorionic plate cells used in this study were within five to nine population doublings (approximately two to five passages).

Reverse transcriptase (RT)-PCR

Chorionic plate cells at PD 6 were dissociated with 0.1% trypsin and 0.25 mM EDTA for 5 min at 37 °C. Total RNA was extracted with RNeasy (Qiagen). Human cardiac RNA was purchased (Clontech). RNA for RT-PCR was converted to cDNA with Superscript (Invitrogen) according to the manufacturer's recommendations. RT-PCR was performed by using primers for the genes of cardiac transcription factors: Csx/Nkx-2.5, GATA4; a cardiac hormone: atrial natriuretic peptide (ANP), brain natriuretic peptide (BNP); cardiac structural proteins: cardiac troponin-I (cTnI), cardiac troponin T (cTnT), myosin light chain-2α (MLC-2α), cardiac actin; and 18s rRNA. 18s rRNA (18S) was used as an internal control. PCR was performed with recombinant Taq (Toyobo Co., Ltd.) or TaKaRa LA Taq with GC Buffer (Takara Shuzo Co., Ltd.) for 30 or 35 cycles, with each cycle consisting of 95 °C for 30 s, 55 °C, 61 °C or 65 °C for 45 s, and 2 °C for 45 s, with an additional 5-min incubation at 72 °C after completion of the final cycle. The PCR was performed in 50 μl of buffer (10 mmol/l Tris–HCl (pH 8.3), 2.5 mmol/l $MgCl_2$, and 50 mmol/l KCl) containing 1 mmol/l each of dATP, dCTP, dGTP, and dTTP, 2.5 U of Gene Taq (Nippon Gene), and 0.2 mol/l primers. The PCR products were size fractionated by 2% agarose gel electrophoresis.

Karyotyping of chorionic plate cells

Metaphase spreads were prepared from chorionic plate cells treated with 100 ng/ml colcemid (Karyo Max, Gibco Co. BRL) for 6 h. We performed karyotyping by G-banding stain on at least 30 metaphase spreads for each population. The CEP X/Y DNA Probe Kit (Vysis) was used to determine the proportion of XX and XY cells in accordance with the manufacturer's suggestions.

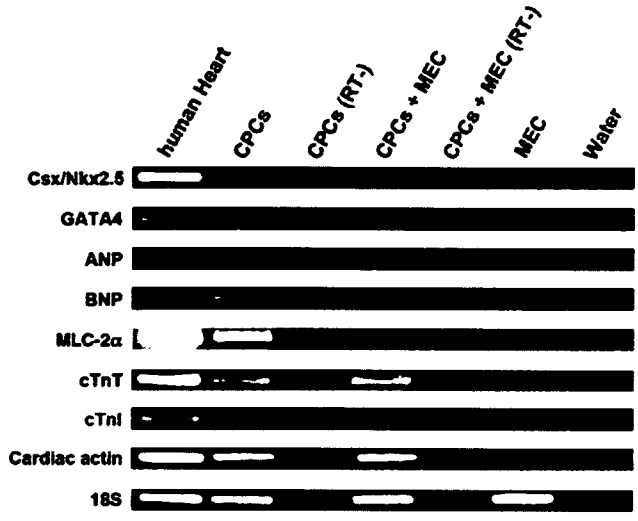

Fig. 2 – Gene expression of cardiomyocyte-specific/associated genes in chorionic plate cells. RT-PCR analysis revealed expression patterns of cardiomyocyte-specific or associated genes; *Csx/Nkx2.5, GATA4, ANP, BNP, cTnI, cTnT, cardiac actin* and *MLC-2α* (from left to right) in human heart, chorionic plate cells (CPCs), chorionic plate cells after co-culturing with murine embryonic cardiomyocytes (CPCs + MEC), murine embryonic cardiomyocytes (MEC) and water. "RT-" represented an omission of a reverse transcriptase treatment to RNA as negative control. Human heart RNA and water (without RNA) served as positive and negative control, respectively. 18s rRNA (18S) was amplified in parallel reactions as a housekeeping gene serving as an internal control.

Flow cytometric analysis

Chorionic plate cells were stained for 1 h at 4 °C with primary antibodies and immunofluorescent secondary antibodies. The cells were then analyzed on a Cytomics FC 500 (Beckman Coulter, Inc.) and the data were analyzed with the FlowJo Ver.7 (Tree Star, Inc.). Antibodies against human CD14 (6603511, Beckman Coulter), CD29 (Integrin-β1) (6604105, Beckman Coulter), CD31 (PECAM-1) (IM1431, Beckman Coulter), CD34 (IM1250, Beckman Coulter), CD44 (IM1219, Beckman Coulter, IM1219), CD45 (556828, Beckman Coulter), CD59 (IM3457, Beckman Coulter), CD73 (550257, BD Pharmingen), CD90 (Thy-1) (555596, BD Pharmingen), CD105 (Endoglin) (A07414, Beckman Coulter) and CD166 (ALCAM) (559263, BD Pharmingen) were adopted as primary antibodies.

Gene chip analysis

Human genomewide gene expression was examined with the Human Genome U133A Probe array (Affymetrix), which contains the oligonucleotide probe set for approximately 23,000 full-length genes and expressed sequence tags (ESTs). Total cellular RNA was immediately isolated with the RNeasy (Qiagen), according to the manufacture's instructions. Contaminating DNA was eliminated by DNase I (Takara Bio Inc.). The purity of RNA was assessed on the basis of the A260/A280 ratio, and the integrity of RNA was verified by agarose gel electrophoresis. Double-stranded cDNA was synthesized from DNase-treated total RNA, and the cDNA was subjected to in vitro transcription in the presence of biotinylated nucleoside triphosphates, according to the manufacturer's protocol (One-Cycle Target Labeling and Control Reagent package [http://www.affymetrix.com/support/technical/manual/expression_manual.affx]). The biotinylated cRNA was hybridized with a probe array for 16 h at 45 °C, and the hybridized biotinylated cRNA was stained with streptavidin-PE and scanned with a Hewlett-Packard Gene Array Scanner (Palo Alto). The fluorescence intensity of each probe was quantified by using the GeneChip Analysis Suite 5.0 computer program (Affymetrix). The expression level of a single mRNA was determined as the average fluorescence intensity among the intensities obtained with 11 paired (perfectly matched and single-nucleotide-mismatched) probes consisting of 25-mer oligonucleotides. If the intensities of mismatched probes were very high, gene expression was judged to be absent, even if high average fluorescence was obtained with the GeneChip Analysis Suite 5.0 program. The level of gene expression was determined with the GeneChip software as the average difference (AD). Specific AD levels were then calculated as the percentage of the mean AD level of six probe sets for housekeeping genes (*actin* and *GAPDH* [glyceraldehyde-3-phosphate dehydrogenase] genes). Further data analysis was performed with Genespring software version 5 (Silicon Genetics). To normalize the staining intensity variations among chips, the AD values for all genes on a given chip were divided by the median of all measurements on that chip. To eliminate changes within the range of background noise and to select the most differentially expressed genes, data were used only if the raw data values were less than 100 AD and gene expression was judged to be present by the Affymetrix data analysis.

Table 1 – RT-PCR primers used in this study

	Primer (sense)	Primer (anti-sense)	Annealing temperature (°C)	Product size (bp)
Csx/Nkx-2.5	CTTCAAGCCAGAGGCCTACG	CCGCCTCTGTCTTCTCCAGC	61	233
GATA4	GACGGGTCACTATCTGTGCAAC	AGACATCGGCACTGACTGAGAAC	61	475
ANP	GAACCAGAGGGGAGAGACAGAG	CCCTCAGCTTGCTTTTTAGGAG	55	406
BNP	CATTTGCAGGGCAAACTGTC	CATCTTCCTCCCAAAGCAGC	55	206
MLC-2α	GAAGGTGAGTGTCCCAGAGG	ACAGAGTTTATTGAGGTGCCCC	65	376
cTnT	GGCAGCGGAAGAGGATGCTGAA	GAGGCACCAAGTTGGGCATGAACGA	65	152
cTnI	CCCTGCACCAGCCCCAATCAGA	CGAAGCCCAGCCCGGTCAACT	65	233
Cardiac actin	CTTCCGGTGTCCTGAGACAC	CCTGACTGGAAGGTAGATGG	61	400
18S	GTGGAGCGATTTGTCTGGTT	CGCTGAGCCAGTCAGTGTAG	55	200

Table 2 – Human cardiomyocyte-specific or -associated gene expression profiling of undifferentiated and differentiated chorionic plate cells (CPCs)

Systematic	Common	Undifferentiated CPCs		Differentiated CPCs		Human heart	Description
207317_s_at	CASQ2	34	A	12	A	P	Calsequestrin 2 (cardiac muscle)
205553_s_at	CSRP3	8	A	5	A	P	Cysteine and glycine-rich protein 3 (cardiac LIM protein)
208040_s_at	MYBPC3	56	A	117	A	P	Myosin binding protein C, cardiac
214468_at	MYH6	11	A	50	A	P	Myosin, heavy polypeptide 6, cardiac muscle, alpha (cardiomyopathy, hypertrophic 1)
204737_s_at	MYH7	5	A	161	P	P	Myosin, heavy polypeptide 7, cardiac muscle, beta
216265_x_at	MYH7	36	A	232	A	P	Myosin, heavy polypeptide 7, cardiac muscle, beta
215795_at	MYH7B	89	A	11	A	P	Myosin, heavy polypeptide 7B, cardiac muscle, beta
209742_s_at	MYL2	267	A	153	A	P	Myosin, light polypeptide 2, regulatory, cardiac, slow
210088_x_at	MYL4	338	P	404	A	P	Myosin, light polypeptide 4, alkali; atrial, embryonic
210395_x_at	MYL4	220	P	412	P	P	Myosin, light polypeptide 4, alkali; atrial, embryonic
219942_at	MYL7	9	A	16	A	P	Myosin, light polypeptide 7, regulatory
207557_s_at	RYR2	11	A	13	A	P	Ryanodine receptor 2 (cardiac)
214044_at	RYR2	17	A	23	A	P	Ryanodine receptor 2 (cardiac)
205742_at	TNNI3	96	A	195	A	P	Troponin I, cardiac
215389_s_at	TNNT2	83	A	165	A	P	Troponin T2, cardiac
205132_at	ACTC	289	P	671	P	P	Actin, alpha, cardiac muscle
206029_at	ANKRD1	214	P	13	A	P	Ankyrin repeat domain 1 (cardiac muscle)
213738_s_at	ATP5A1	5905	P	2657	P	P	ATP synthase, H^+ transporting, mitochondrial F1 complex, alpha subunit, isoform 1, cardiac muscle
205444_at	ATP2A1	107	A	53	A	A	ATPase, Ca^{++} transporting, cardiac muscle, fast twitch 1
209186_at	ATP2A2(SERCA2A)	4465	P	2577	P	P	ATPase, Ca^{++} transporting, cardiac muscle, slow twitch 2
212361_s_at	ATP2A2(SERCA2A)	814	P	338	A	P	ATPase, Ca^{++} transporting, cardiac muscle, slow twitch 2
212362_at	ATP2A2(SERCA2A)	178	P	60	A	A	ATPase, Ca^{++} transporting, cardiac muscle, slow twitch 2
207317_s_at	CASQ2	34	A	12	A	P	Calsequestrin 2 (cardiac muscle)
65472_at		6	A	17	A	A	qb80a04.x1 Soares_fetal_heart_NbHH19W *Homo Sapiens* cDNA clone IMAGE:1706382 3′ similar to TR:O21123 O21123 CYTOCHROME OXIDASE I; mRNA sequence
205298_s_at	BTN2A2	482	P	183	A	A	zd240d07.s1 Soares_fetal_heart_NbHH19W *Homo sapiens* cDNA clone IMAGE:341581 3′, mRNA sequence
213121_at	SNRP70	66	A	6	A	A	zd39c08.s1 Soares_fetal_heart_NbHH19W *Homo sapiens* cDNA clone IMAGE:343022 3′, mRNA sequence
65521_at	LOC51619	658	A	266	A	P	zd56g04.r1 Soares_fetal_heart_NbHH19W *Homo sapiens* cDNA clone IMAGE:344694 5′, mRNA sequence

214014_at	CDC42EP2	38	A	14	A	A	zd85d03.s1 Soares_fetal_heart_NbHH19W *Homo sapiens* cDNA clone IMAGE:347429 3', mRNA sequence
201204_s_at	RRBP1	2174	P	1257	P	P	zf44f12.s1 Soares_fetal_heart_NbHH19W *Homo sapiens* cDNA clone IMAGE:379823 3', mRNA sequence
209331_s_at	MAX	561	P	294	P	P	zg72g05.s1 Soares_fetal_heart_NbHH19W *Homo sapiens* cDNA clone IMAGE:398936 3', mRNA sequence
214776_x_at	XYLB	24	A	13	A	A	zi99g02.s1 Soares_fetal_liver_spleen_1NFLS_S1 *Homo sapiens* cDNA clone IMAGE:448946 3', mRNA sequence
211715_s_at	BDH	59	A	8	A	P	3-hydroxybutyrate dehydrogenase (heart, mitochondrial)
205534_at	PCDH7	8	A	205	P	A	BH-protocadherin (brain–heart)
205535_s_at	PCDH7	7	A	75	P	P	BH-protocadherin (brain–heart)
210273_at	PCDH7	157	A	168	A	P	BH-protocadherin (brain–heart)
210941_at	PCDH7	14	A	3	A	A	BH-protocadherin (brain–heart)
204726_at	CDH13	172	P	195	P	P	Cadherin 13, H-cadherin (heart)
203020_at	HHL	210	P	117	P	P	Expressed in hematopoietic cells, heart, liver
213982_s_at	HHL	335	P	74	P	P	Expressed in hematopoietic cells, heart, liver
205738_s_at	FABP3	79	A	92	P	P	Fatty acid binding protein 3, muscle and heart (mammary-derived growth inhibitor)
214285_at	FABP3	22	A	49	A	P	Fatty acid binding protein 3, muscle and heart (mammary-derived growth inhibitor)
220138_at	HAND1	246	A	117	A	P	Heart and neural crest derivatives expressed 1
220480_at	HAND2	19	A	29	A	A	Heart and neural crest derivatives expressed 2
213036_x_at	ATP2A3	23	A	25	A	A	*Homo sapiens* SERCA3 gene, exons 1–7 (and joined CDS)
204938_s_at	PLN	22	A	60	A	P	Phospholamban
204939_s_at	PLN	71	A	99	A	P	Phospholamban
204940_at	PLN	46	A	28	A	P	Phospholamban
206578_at	NKX2-5	40	A	14	A	P	NK2 transcription factor related, locus 5 (*Drosophila*)
205517_at	GATA4	16	A	46	A	P	GATA binding protein 4
201667_at	GJA1	4792	P	2016	P	P	Gap junction protein, alpha 1, 43 kDa (connexin 43)
208636_at	ACTN1	7896	P	3182	P	P	Actinin, alpha 1
208637_x_at	ACTN1	5400	P	2359	P	P	Actinin, alpha 1
211160_x_at	ACTN1	5727	P	1529	P	A	Actinin, alpha 1
203861_s_at	ACTN2	38	A	17	A	P	Actinin, alpha 2
203862_s_at	ACTN2	53	A	16	A	P	Actinin, alpha 2
203863_at	ACTN2	35	A	20	A	P	Actinin, alpha 2
203864_s_at	ACTN2	189	A	123	A	P	Actinin, alpha 2
206891_at	ACTN3	134	M	133	A	M	Actinin, alpha 3
200601_at	ACTN4	1134	P	282	P	P	Human non-muscle alpha-actinin mRNA, complete cds
211805_s_at	SLCBA1(NCX1)	53	A	228	A	P	Solute carrier family 8 (sodium/calcium exchanger), member 1
207413_s_at	SCN5A	32	A	61	A	P	Sodium channel, voltage-gated, type V, alpha (long QT syndrome 3)

Introduction of the EGFP gene

Recombinant adenovirus carrying the enhanced green fluorescent protein (EGFP) gene was prepared as described [13]. Chorionic plate cells were plated on dishes at $2\times10^5/cm^2$, and infected with EGFP-expressing adenovirus at 10 plaque-forming units/cell on the next day. Chorionic plate cells were examined in vitro by fluorescent confocal microscopy for expression of the EGFP gene. By 7 days post-infection, nearly all of the cells expressed EGFP. To eliminate the possibility of free adenovirus in the cell supernatant, we infected murine fetal cardiomyocytes with chorionic plate cell supernatants after infection. No murine fetal cardiomyocytes expressed EGFP, implying that the cells are not transfected with free adenovirus.

Preparation of murine fetal cardiomyocytes

Fetal cardiomyocytes were obtained from the hearts of day 17 mouse fetuses. The hearts were minced with scissors and washed with PBS, and then incubated in PBS with 0.1% trypsin and 0.25 mM EDTA for 10 min at 37 °C. After DMEM supplemented with 10% FBS was added, the cardiomyocytes were centrifuged at 1000 rpm for 5 min. The pellet was then re-suspended in 10 ml of DMEM with 10% FBS and incubated on glass dishes for 1 h to separate the cardiomyocytes from fibroblasts. The floating cardiomyocytes were collected and re-plated at $5\times10^4/cm^2$.

Co-culture system of chorionic plate cells and murine fetal cardiomyocytes

Neither 5-azaC [12] nor oxytocin [21] was used in this process as they are known to initiate cardiomyogenic differentiation. EGFP-labeled chorionic plate cells were harvested with 0.25% trypsin and 1 mM EDTA and overlaid onto the cultured fetal cardiomyocytes at $7\times10^3/cm^2$. Every 2 days the culture medium was replaced with fresh culture medium that was supplemented with 10% FBS and 1 μg/ml Amphotericin B (Gibco). The morphology of the beating EGFP-labeled chorionic plate cells was evaluated under a fluorescent microscope. The image was monitored using a CCD camera and stored as digital video. The cell contraction was analyzed using an image-edge detection program made by Igor Pro 4 (Wavemetrics Inc., Lake Oswego, Oregon).

Electrophysiological analysis

On day 10 of co-cultivation, action potentials (APs) were recorded as described previously [12,13] from spontaneously beating EGFP-labeled cells. Spontaneously beating EGFP-positive chorionic plate cells were selected as targets. The APs of the targeted cells had been recorded and Alexa568 dye was injected by iontophoresis to confirm that the APs were generated by EGFP-positive chorionic plate cells. The extent of dye transfer was monitored under a fluorescence microscope, and digital images were recorded with a digital photo camera (D100; Nikon, Tokyo, Japan) mounted on a microscope with a fluorescence filter (UMWIG2; Olympus).

Immunocytochemistry

A laser confocal microscope (LSM510, Zeiss) was used for immunocytochemical analysis. The chorionic plate cells co-cultured with fetal cardiomyocytes in vitro were fixed with 2% paraformaldehyde (PFA) in PBS for 20 min at 4 °C and treated with 0.1% Triton-X PBS for 20 min at room temperature. These cells were then stained with mouse monoclonal anti-human cardiac troponin-I antibody (#4T21/19-C7 HyTest, Euro, Finland) diluted 1:300, monoclonal anti-α-actinin antibody (Sigma) diluted 1:300, and anti-connexin 43 antibody (Sigma) diluted 1:300. To prevent fading and to stain nuclei, a Slow Fade Light Antifade kit with 4′-6-diamidino-2-phenylindole (DAPI) (Molecular Probes) was used.

Results

Establishment of chorionic plate cells

Almost all human tissues or organs can be a source of MSCs, which have been extracted from fat, muscle, menstrual blood, endometrium, placenta, umbilical cord, cord blood, skin, and eye. In this study, we focused on cells derived from fetuses, since fetus-derived cells tend to both differentiate and proliferate better than adult cells [22]. In that sense, human placenta is a good source of fetus-derived MSCs. We cultivated chorionic plate cells that were obtained from the chorionic mesoderm of the placenta (Fig. 1A). The chorionic plate cells regarded as being Population Doubling (PD) 0 or Day 0 were fibroblast-like in morphology, indistinguishable in appearance from the marrow-derived MSCs, and relatively larger in size than rapidly self-renewing stem cells [23] (Fig. 1B). The cells from PD 9 to PD 18 rapidly proliferated in culture and were propagated continuously. Chorionic plate cells did not undergo malignant transformation. They stopped dividing after reaching confluence and they did not form any foci after reaching confluence in vitro.

To clarify the character of the established chorionic plate cells, we first performed karyotypic analysis of 30 cells at PD 3. All cells had normal chromosomes without any chromosomal aberration (Fig. 1C). The sex chromosomes were found to be XY, implying that all cells were of fetal origin. Genomic FISH analysis also revealed that all cells had XY chromosomes (Fig. 1D). We examined the cell surface marker of the placenta-derived cells (chorionic plate cells) by FACS analysis (Fig. 1E). The surface markers of chorionic plate cells are exactly the same as those of previously reported bone-marrow- and cord blood-derived mesodermal cells, i.e., positive for CD29, CD44,

Fig. 3 – Immunocytochemistry of chorionic plate cells for human cardiac troponin-I. (A–F) Immunocytochemistry of differentiated chorionic plate cells with anti-human cardiac troponin-I (cTnI) antibody. The EGFP-positive cells (B) were stained with anti-human cTnI antibody (A) and the merged image (DAPI, EGFP, cTnI) is shown in panels D and F. An enlarged image (red square in D) is shown in panel E. Clear striations were observed with red fluorescence of cTnI in the differentiated cells. (G–I) A merged image for EGFP and cTnI is shown in panel G. A longitudinal section at the green line in the merged image G is shown in panel H. An axial section at the red line in merged image G is shown in panel I.